Journal of Nuclear Materials 464 (2015) 342–345

Contents lists available at ScienceDirect

Journal of Nuclear Materials

journal homepage: www.elsevier.com/locate/jnucmat

Letter to the Editor

High-temperature corrosion behavior of Ni–16Mo–7Cr–4Fe superalloy containing yttrium in molten LiF–NaF–KF salt

Xiao-li Li, Shang-ming He *, Xing-tai Zhou, Ping Huai, Zhi-jun Li, Ai-guo Li, Xiao-han Yu *

Shanghai Institute of Applied Physics, China Academy of Sciences, Shanghai 201800, PR China

HIGHLIGHTS

- Traces of yttrium were doped in Ni–16Mo–7Cr–4Fe nickel-base superalloy.
- High-temperature corrosion resistance is improved by proper yttrium addition.
- Synchrotron radiation X-ray fluorescence with high sensitivity was adopted.

ARTICLE INFO

Article history:
Received 26 January 2015
Accepted 9 May 2015
Available online 21 May 2015

ABSTRACT

The corrosion tests of a Ni–16Mo–7Cr–4Fe superalloy containing various yttrium contents were performed in molten FLiNaK (LiF–NaF–KF: 46.5–11.5–42 mol%) salt at 850 °C for 620 h, with the goals of investigating the effects of yttrium on the corrosion resistance of Ni–16Mo–7Cr–4Fe alloy and understanding the corrosion mechanisms. The addition of an appropriate amount of yttrium promotes the formation of a Y-rich layer near the surface and inhibits the diffusion of the susceptive elements.

1. Introduction

Molten fluoride salts have been proposed for use as primary and secondary reactor coolants, media for transfer of high temperature process heat from nuclear reactors to chemical plants [1], and for concentrated solar power thermal energy storage. The cooling of Thorium Molten Salt Reactor (TMSR) with the molten salts, however, brings new problems connected with high temperature corrosion. In molten fluoride salts the surface scale of alloys are chemically unstable, and corrosion is driven largely by the thermodynamically driven dissolution of alloying elements into the molten salt environment [2–4].

So far, much effort has been devoted to the study of the corrosion of alloys in molten salts [5–7]. However, little work focused on the molten corrosion behavior of the Ni-based superalloy containing trace amounts of yttrium. Yttrium has been applied successfully in many fields such as metallurgy and chemical and surface engineering [8]. Some reports exist on yttrium modification in the nickel-base alloys [9–12]. Yttrium can improve many properties, such as the oxidation resistance of alloys [9], the creep property of cast stainless steels [10], the stress rupture of nickel-based superalloys [11,12] and so on. This paper deals with the effects of yttrium on the corrosion resistance of Ni–16Mo–7Cr–4Fe alloy containing various yttrium contents after their exposure to the molten FLiNaK (LiF–NaF–KF: 46.5–11.5–42 mol%) salt at 850 °C for 620 h, and the influence mechanism is also discussed. This research can help extend the usable critical temperature of nickel-based superalloys for the Molten Salt Energy System.

2. Experimental

Specimens ($2 \times 10 \times 30\ mm^3$) G00, G05, G10, G30 and G50 are the Ni–16Mo–7Cr–4Fe alloy with the addition of 0.00, 0.05, 0.10, 0.30 and 0.50 (in wt%) of yttrium. The chemical composition of Ni–16Mo–7Cr–4Fe alloy supplied by Institute of Metal Research in Shenyang is shown in Table 1. FLiNaK (LiF–NaF–KF: 46.5–11.5–42 mol%) salt was selected for this research. The corrosion tests were performed in the sealed graphite crucibles under an argon cover gas. To ensure the salt purity, the graphite crucibles were encapsulated in an outer 304 stainless steel containment and welded shut [13]. The FLiNaK salt was put into the crucibles inside an argon atmosphere glove box. The volume occupied by the molten salt may be calculated as a function of temperature from its density (in units of kg/m^3) using the relationship: $\rho = 2530–0.73T$ [1]. Then the crucibles were heated up to 850 °C in a furnace and maintained at 850 °C for 620 h. After the 620 h exposure, the corrosive specimens were cleaned of the residual salt

* Corresponding authors. Tel./fax: +86 21 33933227 (S.-m. He). Tel./fax: +86 21 39194703 (X.-h. Yu).
E-mail addresses: heshangming@sinap.ac.cn (S.-m. He), yuxiaohan@sinap.ac.cn (X.-h. Yu).

http://dx.doi.org/10.1016/j.jnucmat.2015.05.007
0022-3115/

Table 1
Chemical composition of Ni–16Mo–7Cr–4Fe alloy (wt%).

Mo	Cr	Fe	Mn	Si	Al	Ti	Cu	C	Ni
16.10	7.32	4.15	0.41	<0.002	0.11	<0.002	0.002	0.038	Bal

using 1 mol/L $Al(NO_3)_3$ according to the method used by Olson et al. [14].

3. Results and discussion

Among the five tested alloys, the weight loss of G05 is the lowest, nevertheless, the weight loss increases with further increasing yttrium addition to a value even higher than that of G00, as shown in Fig. 1. The large variation of the weight loss among the five tested alloys, demonstrates the complex roles of yttrium playing in the corrosion susceptibility. The addition of an appropriate amount of yttrium is beneficial to the molten corrosion resistance, but excess yttrium additions are detrimental to the corrosion resistance. The five alloys exposed to the FLiNaK salt show void formation to varying depths (Fig. 2). The void formation accompanies the Cr and Fe depletion. All of the tested alloys show selective leaching of Cr and Fe. The chromium gradient extends approximately 20 μm to the surface of the alloys G00 and G50; however, the corrosion layer of G05 is just several micrometers (Figs. 2 and 3).

In the Ni–16Mo–7Cr–4Fe alloys Cr and Fe are the less noble components and can be expected to be selectively removed, and Mo and Ni are generally resistant to dissolution in the FLiNaK salt. The Gibbs free energy of formation per molecule of F_2 for the salt constituents and the metal fluorides formed from the tested alloys at 850 °C, calculated using HSC Chemistry 6.0 computer software and its associated database, can be ranked by decreasing stability [15]:

$$MoF_6 > MoF_3 > NiF_2 > FeF_3 > FeF_2 > CrF_3 > CrF_2 > MnF_2 > KF > NaF > YF_3 > LiF.$$

For example, the chromium depletion in Ni–16Mo–7Cr–4Fe alloys occurs through formation of chemical compounds at the surface with subsequent removal of Cr in the matrix, leaving a depleted zone.

A driving force exists for chromium to react with the impurities in the fluoride mixture:

$$Cr + NiO = CrO + Ni$$

$$Cr + NiF_2 \ (\text{or } FeF_2) = CrF_2 + Ni \ (\text{or } Fe)$$

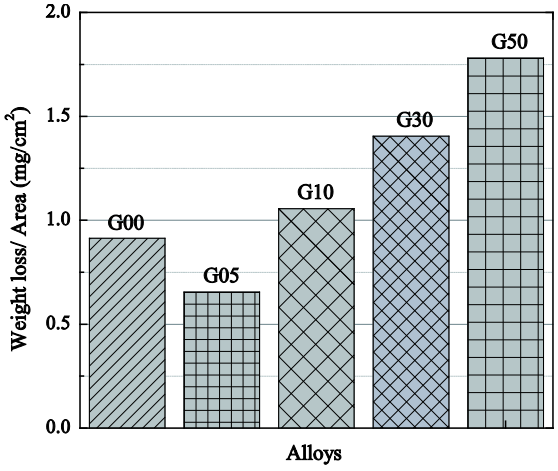

Fig. 1. Weight-loss due to the corrosion of the tested alloys after exposure to the FLiNaK salt at 850 °C for 620 h.

Another driving force exists for chromium to react with the fluoride mixture:

$$xA(s) + yBF(l) = A_XF_Y(l) + yB(l) \quad (A = Fe, Ni, Cr; B = Li, Na, K)$$

The void formation arises from the Kirkendall effect, in which solute atoms of a given type diffuse out faster than other atoms from the crystal lattice can diffuse into fill the resulting vacancies. The corrosion in the molten salt is somewhat unique since in general no protective film is formed to prevent further dissolution. Various corrosion products can be dissolved in the molten FLiNaK salt. However, a Y-rich layer is observed near the surface of the corrosion layer in alloy G05 (Fig. 2e), which is not observed in the other tested alloys. Synchrotron Radiation X-ray fluorescence (SRXRF) mapping analyses performed on the cross section of Ni–16Mo–7Cr–4Fe alloys were also conducted, showing a reasonably uniform depletion of Cr and Fe and confirming that Mo and Ni are generally resistant to dissolution in the FLiNaK salt (Fig. 3). The SRXRF analyses are consistence with the SEM results, showing yttrium tends to accumulate near the surface of the corrosion layer and form a Y-rich layer in alloy G05 (Fig. 3b), but the Y-rich layer was not observed in alloy G10, G30 and G50. The Y accumulation effect is related to the concentration of yttrium in the matrix. For these alloys containing excess yttrium, the addition amount of Y in the alloys is very small and most of yttrium in the matrix is consumed to form stable $Ni_{17}Y_2$ phase [16]. In comparison, the Y concentration in the matrix of G05 is the highest among the five tested alloys and there is enough yttrium to form the successive Y-rich layer. Furthermore, both grazing incidence X-ray diffraction (GIXRD) analyses and the XPS result of the G05 corrosion scale show that the Y-rich layer appears in alloy G05 and the Y-rich layer contains YF_3 (Fig. 4a and b), confirming that Y is a very reactive element and easy to combine with F. Moreover, the result of Inductively Coupled Plasma-Atomic Emission Spectroscopy (ICP-AES) shows that the concentrations of Cr and Fe in the FLiNaK salt after the corrosion tests reach its minimum at 0.05 wt% Y addition content and then increase obviously with further increasing Y addition (Fig. 5). It can be speculated that the Y-rich layer inhibits the diffusion of Cr and Fe from the inner alloy to the surface and thus decreases the salt corrosion effectively. Consequently, Y was not selectively removed but formed a successively compact Y-rich layer at the surface of alloy G05. The alloys without Y and containing excess Y exhibits the severer corrosion than Ni–16Mo–7Cr–4Fe alloy added with 0.05 wt% Y.

Another unignorable influence factor is the size, distribution and number of Mo-rich carbide particles, which exist in all the tested alloys (Fig. 2). The Mo-rich carbide particles are small and distribute both at grain boundaries and in grain interior for alloy G05; however, the carbide particles are coarse and mainly distribute at grain boundaries for the other tested alloys, especially for alloy G50 which contains too much yttrium. The coarse carbide particles have a large carbide/matrix interface connected to grain boundaries, which provide fast diffusion paths for the susceptive elements. There is also a possibility for the coarse carbide particles and the matrix to form a galvanic couple at surface, which cause additional galvanic corrosion. Eventually, the alloys containing excess Y suffer the severe corrosion.

4. Conclusions

Cr and Fe dissolution in the molten FLiNaK salt are the main reasons for the corrosion of the Ni–16Mo–7Cr–4Fe alloys. The addition of an appropriate amount of yttrium modifies the FLiNaK salt corrosion resistance of Ni–16Mo–7Cr–4Fe alloy by forming the Y-rich layer, which can impede the dissolution of Cr and Fe. However, excess Y addition is detrimental to the salt corrosion resistance.

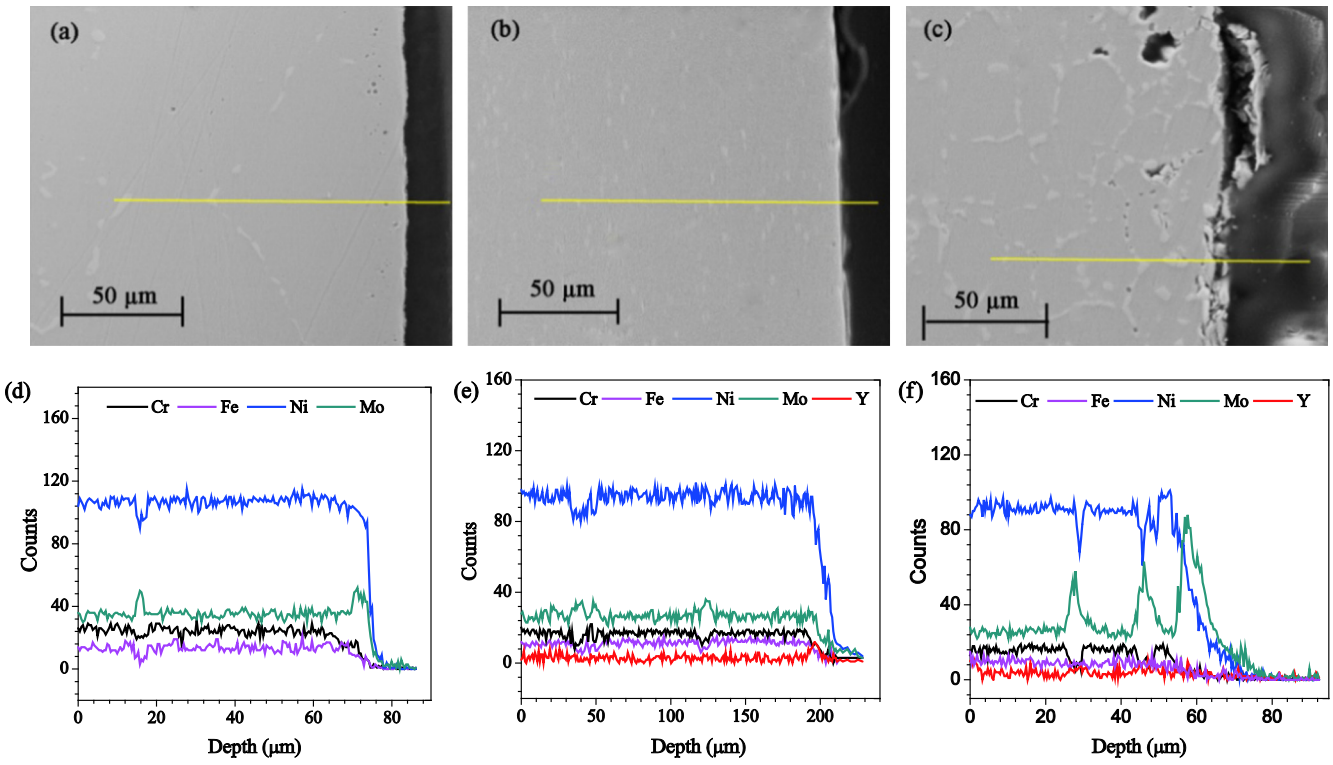

Fig. 2. Cross-sectional SEM images and line scan EDS analyses of the corrosion layer of the tested alloys after the corrosion tests in FLiNaK salt at 850 °C for 620 h. (a) G00, (b) G05, (c) G50, (d) EDS of G00, (e) EDS of G05, (f) EDS of G50.

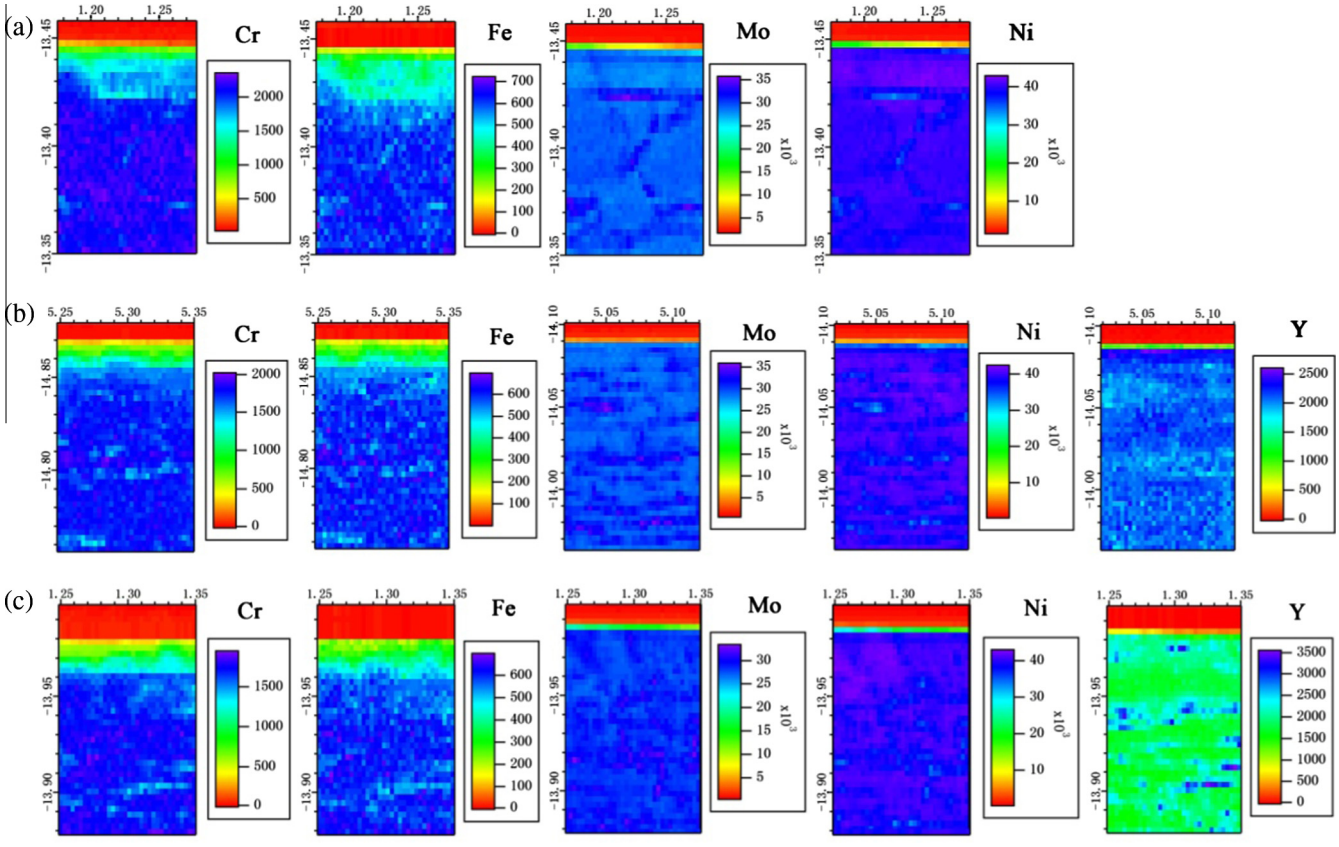

Fig. 3. Cross-sectional XRF mapping of the tested alloys after exposure in the FLiNaK salt at 850 °C for 620 h. (a) G00, (b) G05, (c) G50.

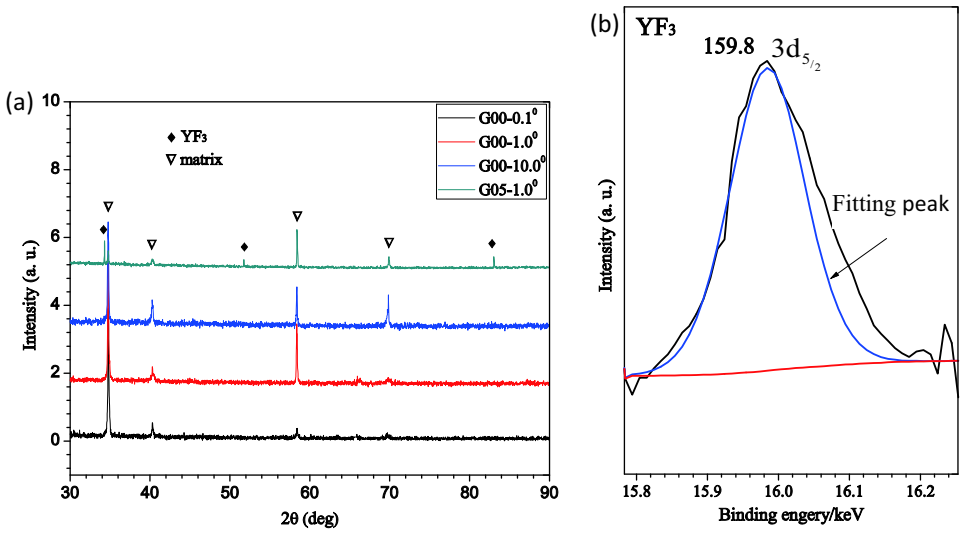

Fig. 4. Spectra of the corrosion layer: (a) GIXRD of G00 and G05 and (b) XPS of Y $3d_{5/2}$ peak of G05.

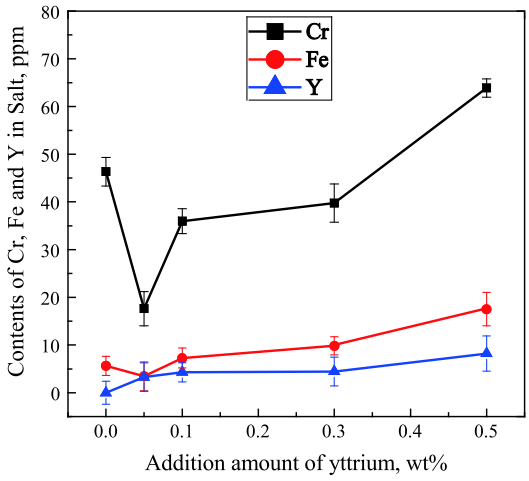

Fig. 5. The contents of Cr, Fe and Y in the FLiNaK salt after the corrosion tests determined by ICP-AES as a function of Y addition contents of Ni–16Mo–7Cr–4Fe alloy (Weight ppm).

Acknowledgements

This work is financially supported by the Program of International S&T Cooperation Grant (No. 2014DFG60230), the National Natural Science Foundation of China (Nos. 51371189 and 51371188). The authors also wish to thank Beamline BL 15U1 of SSRF.

References

[1] C.B. Xiao, Y.F. Han, Scr. Mater. 41 (1999) 475–480.
[2] J. Kudrman, J. Cmakal, I. Nedbal, J. Siegl, Kov Mater-Met Mater. 38 (2000) 29–42.
[3] J. Kudrman, J. Cmakal, I. Nedbal, J. Siegl, Kov Mater-Met Mater. 37 (1999) 412–423.
[4] L. Olson, K. Sridharan, M. Anderson, T. Allen, J. Nucl. Mater. 411 (2011) 51–59.
[5] Lubomír Král, Jiří Čermák, Oldřich Matal, Tomáš Šimo, Lukáš Nesvadba, Metal (2010) 1–5.
[6] D.F. Williams, ORNL/TM-2006/69, Oak Ridge National Laboratory, 2006.
[7] D.F. Williams LMT, K.T. ORNL/TM-2006/12, Oka Ridge National Laboratory, 2006.
[8] S.X. Wang, C. Li, B.J. Xiong, X.B. Tian, S.Q. Yang, Appl. Surf. Sci. 257 (2011) 5826–5830.
[9] F.H. Stott, G.C. Wood, J.G. Fountain, Oxid. Met. 14 (1980) 135–146.
[10] C.B. Xiao, Y.F. Han, Scr. Mater. 41 (1999) 1217–1221.
[11] P.J. Zhou, J.J. Yu, X.F. Sun, H.R. Guan, X.M. He, Z.Q. Hu, Mater. Sci. Eng. A-Struct. Mater. Prop. Microstruct. Process. 551 (2012) 236–240.
[12] P.J. Zhou, J.J. Yu, X.F. Sun, H.R. Guan, Z.Q. Hu, Scr. Mater. 57 (2007) 643–646.
[13] J. Qiu, Y. Zou, G. Yu, H. Liu, Y. Jia, Z. Li, et al., J. Fluorine. Chem. 168 (2014) 69–74.
[14] Luke Olson, Kumar Sridharan, Mark Anderson, Todd Allen, J. Nucl. Mater. 411 (2011) 51–59.
[15] A. Machet, A. Galtayries, S. Zanna, L. Klein, V. Maurice, P. Jolivet, et al., Electrochim. Acta 49 (2004) 3957–3964.
[16] X.L. Li, S.M. He, X.T. Zhou, Y. Zou, Z.J. Li, A.G. Li, et al., Mater. Charact. 95 (2014) 171–179.